

Model experiments on the 100,000-yr glacial cycle

J. Oerlemans*

Royal Netherlands Meteorological Institute, De Bilt, The Netherlands

It is believed that during the Quaternary era changes in global ice volume were mainly due to changes in the size of the ice sheets on the Eurasian and American continents. Time spectra of oxygen isotope records from deep-sea cores and of the Earth's orbital parameters are remarkably similar in the 10,000–120,000-yr range^{1,2}, suggesting that changes in global ice volume are forced by insolation variations. Model studies by Weertman^{3,4} and Pollard⁵ have confirmed this point to some extent: the 20,000- and 40,000-yr cycles can be reproduced, but the 100,000-yr cycle does not show up. Recently, Imbrie and Imbrie⁶ have fitted simple nonlinear mathematical models to $\delta^{18}\text{O}$ curves. They found that reasonable fits are obtained if the time scale for ice-sheet growth is about 27,000 yr and for decay about 7,000 yr. The present study considers the problem of the 100,000-yr cycle in a similar way. Experiments with a Northern Hemisphere ice-sheet model show that the 100,000-yr cycle and its sawtooth shape may be explained by ice sheet/bedrock dynamics alone. This cycle seems to be an internally generated feature and is not forced by variations in the eccentricity of the Earth's orbit.

First, consider the 'classical' record of core V12-122 (Fig. 1). This core has a comparatively high resolution and spans about the last 500,000 yr. Two features that are immediately evident are that the dominant signal is a periodic one, with a period of about 100,000 yr, and that this cycle is strongly asymmetric, having a sawtooth shape. The strong response of the cryosphere on the 100,000-yr time scale, as compared with those on the 20,000- and 40,000-yr time scales, suggests some kind of resonance. Variations in eccentricity of the Earth's orbit may have combined with the internal dynamics of the climate system to create a strong signal in global ice volume.

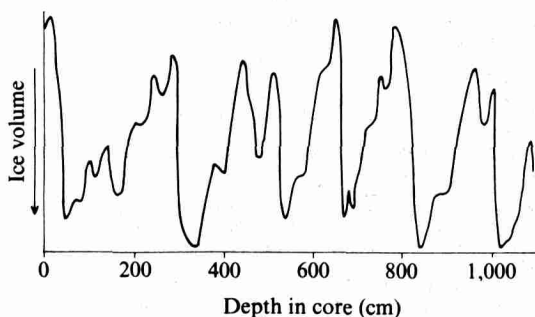


Fig. 1 A plot of the $\delta^{18}\text{O}$ record of the Carribbean core V12-122 (data from ref. 12). According to the 'tune-up' time scale of Hays *et al.*², the glacial maximum found at a depth of 840 cm in this core occurred at 430,000 yr BP. The most pronounced features are the 100,000-yr cycle and the asymmetric shape of these cycles.

Figure 1 suggests that the time needed to create full-size ice sheets is 50,000–100,000 yr, considerably more than has been suggested by theoretical studies^{4,7}. I will discuss some model results indicating that such a growth time scale is in accordance with bedrock/ice sheet dynamics.

The most dramatic feature of Fig. 1 is the speed with which deglaciations seem to take place $\sim 10,000$ yr. Also important is

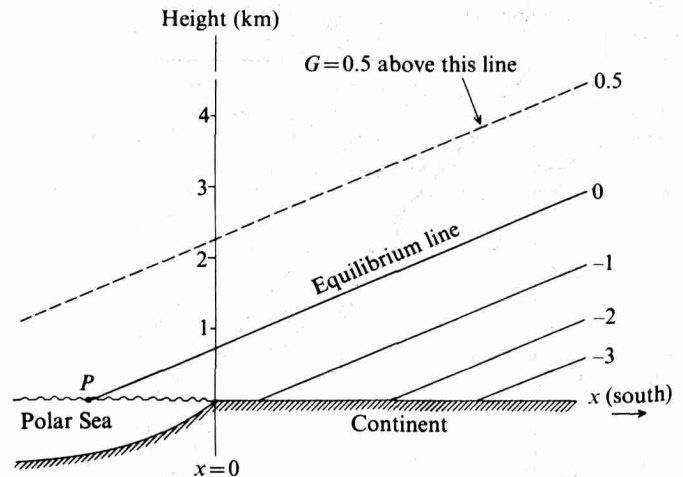


Fig. 2 Mass-balance conditions for a Northern Hemisphere ice sheet, as parameterized in the model. The intersection of the equilibrium line with sea level is called the 'climate point', and is indicated by *P*. Insolation variations are represented by shifting *P* north- and southwards. Values of the constants used are: $a = 0.73 \times 10^{-3} \text{ yr}^{-1}$, $b = 0.27 \times 10^{-6} \text{ m}^{-1} \text{ yr}^{-1}$, $\chi = 0.65 \times 10^{-3}$. Values for *G* are given beside each line.

the fact that just before deglaciation starts, the growth rate of the ice volume does not fall, which indicates that during the glacial maxima the Northern Hemisphere ice sheets were far from equilibrium. Also, the difference in $\delta^{18}\text{O}$ between a glacial minimum and the subsequent maximum is fairly constant, suggesting an inherent instability of the climate system, and probably of the cryosphere.

A mechanism that might explain this instability is bedrock sinking. Weertman⁴ first suggested this as a possible cause for rapid deglaciation in connection with the Northern Hemisphere ice sheets. I will now discuss model experiments which deal with this point.

The Northern Hemisphere ice-sheet model to be used is described by the equations⁸

$$\frac{\partial H}{\partial t} = \frac{\partial}{\partial x} \left[D \frac{\partial (H+h)}{\partial x} \right] + DH/Y^2 + G \quad (1)$$

$$\frac{\partial h}{\partial t} = -\alpha(H+3h) \quad (2)$$

$$G = a(H+h-E) + b(H+h-E)^2 \quad (3)$$

Equation (1) formulates the conservation of ice mass; it is essentially a nonlinear diffusion equation. The diffusivity for ice mass *D* increases monotonically with ice thickness *H* and the slope of the ice surface $\partial(H+h)/\partial x$ (where *h* is the bedrock height with respect to some geopotential level). The *x*-axis points in a southward direction, so the evolution of the ice sheet is explicitly computed along a meridian. The term DH/Y^2 governs lateral ice-mass discharge, where *Y* is a characteristic east-west length scale of the ice sheet. *G* is the mass balance of the sheet, and is a function of height with respect to the equilibrium line [see equation (3)]. The height of the equilibrium line (defined by $G = 0$) is denoted by *E*; it increases linearly with *x* at a rate χ (Fig. 2).

Equation (2) deals crudely with isostatic adjustment of the Earth's crust. In the equilibrium case, $h = -H/3$ corresponds to a rock density of three times that of ice. The time scale of adjustment is given by $1/3\alpha$.

Figure 2 shows in detail the appearance of the mass balance. Insolation variations may be interpreted as shifting the equilibrium line northwards and southwards. During periods with large eccentricity of the Earth's orbit, the amplitude of the 'climate point' *P*, due to precession of the equinoxes, is about 10° in terms of equivalent latitude⁹. Only during such periods does *P* reach the continent; normally, it is located in the Polar Sea.

* Present address: Institut voor Meteorologie en Oceanografie, State University of Utrecht, Princenplein 5, 3508 TA Utrecht, The Netherlands.

If P lies on the continent for some time, an ice sheet will start to grow. Due to the feedback between surface elevation and mass balance the ice sheet may continue to grow even if insolation increases and P returns to the Polar Sea. Bedrock sinking, however, attempts to cancel this feedback.

I have carried out several numerical integrations of equations (1)–(3). The model was solved on a grid with 70 km spacing, the lateral scale Y being 1,000 km. (For more technical detail, see ref. 8.) In the first experiment, a periodic forcing was imposed by varying the position of the climate point according to

$$P = -140 + 490 \times \sin(2\pi t/T) \text{ km} \quad (4)$$

Remember that $P < 0$ implies that P is located in the Polar Sea. T was set to 20,000 yr, so equation (4) roughly represents conditions during maximum eccentricity. The precise form of the forcing function seems to be relatively unimportant—once the ice sheet reaches a height of ~ 500 m, ice-sheet dynamics take over. Thus, the only requirement is that P remains for a sufficient time on the continent. In view of this, our model can be kept simple by using equation (4) as a universal forcing function in this experiment.

Figure 3 shows four model runs with various time scales for isostatic adjustment (T^*). Figure 3a ($T^* = \infty$) shows the case without any movement of the bedrock. The ice sheet grows slowly, then more rapidly, and comes into a stable oscillation with quite small amplitude. A huge increase in the height of the equilibrium line would be required to remove the ice sheet.

Figure 3b and c show what happens if adjustment takes place on time scales of 30,000 and 10,000 yr, respectively. The ice sheet grows at a smaller rate now, and after about 100,000 yr disappears 'spontaneously'. Apparently, the sinking of the

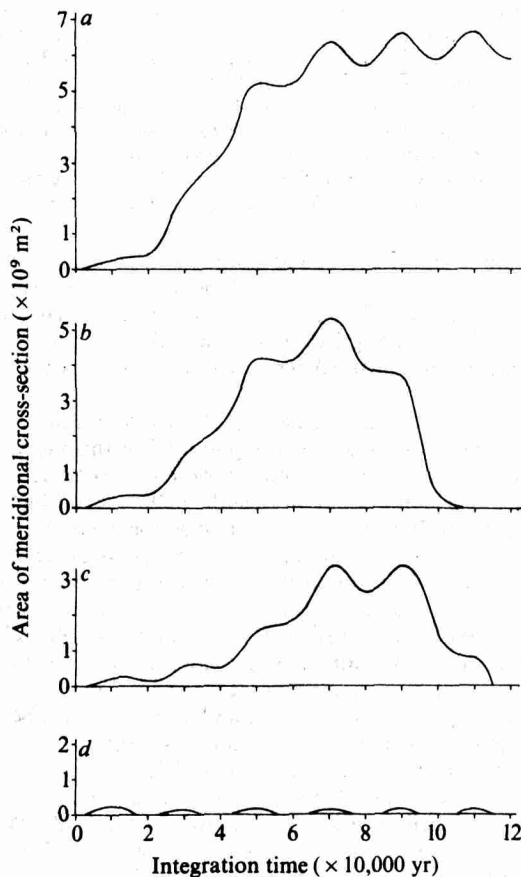


Fig. 3 Model runs with various time scales of isostatic adjustment (T^*). The area of the meridional cross-section through the ice sheet is given along the vertical axis. To obtain the ice-sheet volume, this should be multiplied by a characteristic east-west extent of the sheet. Values for T^* are: a, ∞ ; b, 30,000 yr; c, 10,000 yr; d, 5,000 yr.

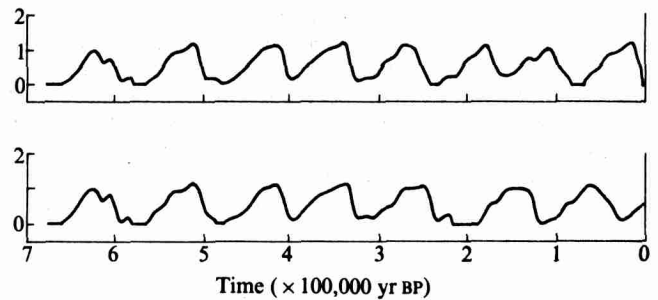


Fig. 4 Two model runs in which the Milankovitch insolation variations are imposed. The vertical axis gives a measure of the ice volume; a value of 1 on the scale corresponds to a meridional ice-sheet size of about 2,000 km and a maximum ice thickness of about 3,000 m. For more details on the parameterization of the mass balance see ref. 9. The only difference between the two runs is the value of T^* , 10,000 and 11,000 yr, respectively, in the upper and lower runs.

bedrock brings a large part of the ice surface beneath the equilibrium line, thus setting the breakdown in motion. Here, significantly, a sawtooth shape appears.

Figure 3d shows the situation when $T^* = 5,000$ yr, so that the isostatic balance is restored very quickly. In this case, the ice sheet cannot grow—the bedrock sinking completely cancels the effect of the height-mass balance feedback.

I next examined the situation in which the model is forced by real insolation variations. These variations were computed from expansions of the orbital parameters given by Berger¹⁰ and translated into mass-balance variations by using an ice/snow melt model⁹. In each of two runs performed, the integration was started at 675,000 yr BP, with initial condition $H(x) = h(x) = 0$.

Figure 4 shows the results. The only difference between the two runs is the value used for the time scale of isostatic adjustment. The agreement in the character of the simulated curves and the $\delta^{18}\text{O}$ record is striking—a 100,000-yr periodicity and an asymmetric shape of the glacial cycles. However, a different situation is obtained with regard to the phase of the cycles. Although dating of the $\delta^{18}\text{O}$ record is in fact not accurate enough to verify the model simulation of all glacial cycles, a comparison of the curves shown in Fig. 4 indicates that the phase of the glacial cycles seems to be extremely sensitive to the model parameters. I believe that this property of the model reflects a realistic feature: the global climatic variations of the Pleistocene seem to have been of a stochastic periodic nature. In view of this, it seems unlikely that the present model can produce an 'in-phase simulation' of the observed ice-volume record, but it does provide a physical explanation for the occurrence of the glacial cycles.

One of the implications of the present results is that the 100,000-yr cycle is mainly internally generated by the interaction of the bedrock adjustment and the height-mass balance feedback. This means that the occurrence of a 100,000-yr peak in the power spectrum of the $\delta^{18}\text{O}$ record² is unrelated to variations in eccentricity. Recent work by Kominz and Pisias¹¹ strongly supports this view: they found that coherence spectra of an oxygen isotope record and the orbital parameters showed no significant peak around a period of 100,000 yr.

Because the present theory deals with two large ice sheets on the Northern Hemisphere continents, it seems unlikely that they can be simulated with exactly the same model parameters. It is possible, however, that the Laurentide ice sheet dominates, and trails the Eurasian one with it through the atmospheric/oceanic teleconnection. Another objection to the theory is the passive role of the Southern Hemisphere. I must stress that the fact that global ice volume seems to lag the Southern Hemisphere sea-ice extent or sea-surface temperature² need not imply that events in the Southern Hemisphere initiate glacial cycles. This may be simply a matter of different response times.

Thus, my main conclusion is that the 100,000-yr cycle can be explained by ice sheet/Earth's crust dynamics, as was suggested by Weertman⁴. Due to bedrock sinking, ice sheets grow very slowly. If the bedrock sinking becomes more substantial, a larger part of the ice surface comes below the equilibrium line, setting the breakdown in motion. Another glacial cycle starts if two conditions are fulfilled—summer insolation should be well below 'normal' and the bedrock should have been raised again.

Received 4 June; accepted 1 August 1980.

1. Van den Heuvel, E. P. *J. Geophys. J. R. astr. Soc.* **11**, 323–336 (1966).
2. Hays, J. D., Imbrie, J. & Shackleton, N. J. *Science* **194**, 1121–1132 (1976).
3. Weertman, J. *Nature* **261**, 17–20 (1976).
4. Weertman, J. *J. geophys. Res.* **78**, 4463–4471 (1961).
5. Pollard, D. *Nature* **272**, 233–235 (1978).
6. Imbrie, J. & Imbrie, J. Z. *Science* **207**, 943–953 (1980).
7. Weertman, J. *J. Glaciol.* **38**, 145–158 (1964).
8. Oerlemans, J. *Tellus* (in the press).
9. Oerlemans, J. & Bienfait, J. M. in *Proc. Sun and Climate Conf.* (CNES, Toulouse, 1980).
10. Berger, A. L. *J. atmos. Sci.* **35**, 2362–2367 (1978).
11. Kominz, M. A. & Pisias, N. G. *Science* **204**, 171–173 (1979).
12. Imbrie, J., Van Donk, J. & Kipp, N. G. *Quat. Res.* **3**, 10–38 (1973).

Carbon-13 in tree-ring cellulose as an indicator of past climates

T. Mazany, J. C. Lerman & A. Long

Laboratory of Isotope Geochemistry, Department of Geosciences, University of Arizona, Tucson, Arizona 85721

Following Urey's suggestion¹ that the ¹³C abundance (usually expressed as a relative ratio: ¹³C/¹²C or $\delta^{13}\text{C}$) fixed in plant carbon may be temperature dependent, several authors have investigated the relationship between $\delta^{13}\text{C}$ and climate. These workers searched for a coefficient relating $\delta^{13}\text{C}$ variations to temperature variations^{2–7}. The results, obtained on field collected samples, failed to yield agreement about the extent of a climatic effect or even its existence. Growth chamber experiments, performed on different plant species in controlled conditions to eliminate environmental factors other than temperature, showed no clear relationship between $\delta^{13}\text{C}$ and temperature^{8,9}. These various contradictory results suggest that factors other than temperature contribute to determining $\delta^{13}\text{C}$ in plants. We now present evidence that the variations of the relative abundance of stable isotopes of carbon in tree rings indicate past climate changes. Thus carbon isotope composition appears to be a proxy indicator that may help to extend the meteorological data base into pre-instrument times.

To gain a better understanding of the relationship between $\delta^{13}\text{C}$ values in tree rings and climate, we analysed two dendrochronologically-dated tree sections collected at Chetro Ketl, an archaeological site in Chaco Canyon, New Mexico. These samples, one, of ponderosa pine (*Pinus ponderosa*) dating from AD 810 to 1045 (sample CK-713), the other, a white fir (*Abies concolor*) dating from AD 931 to 1047 (sample CK-857), were provided by the Laboratory of Tree-Ring Research at the University of Arizona. Tree-ring material was chosen for the experiments because it can be absolutely dated, and, in this case, tree-ring width variations provided information on climate variations with which to correlate our isotope data. These variations are derived from the regional tree-ring chronologies for Chaco Canyon, of which there is one for ponderosa pine and one for white fir^{10,11}. The dendrochronological record is obtained by standardizing the ring widths of each one of several trees in one region, forming ring-width indices, with a mean value of 1.0 (see refs 10–12). These indices are averaged over the several individual trees to obtain the regional tree-ring chronology, which is given as a time series of mean standardized ring-width indices^{12–14}. This filters the growth effects experienced by individual trees, while preserving climatically induced varia-

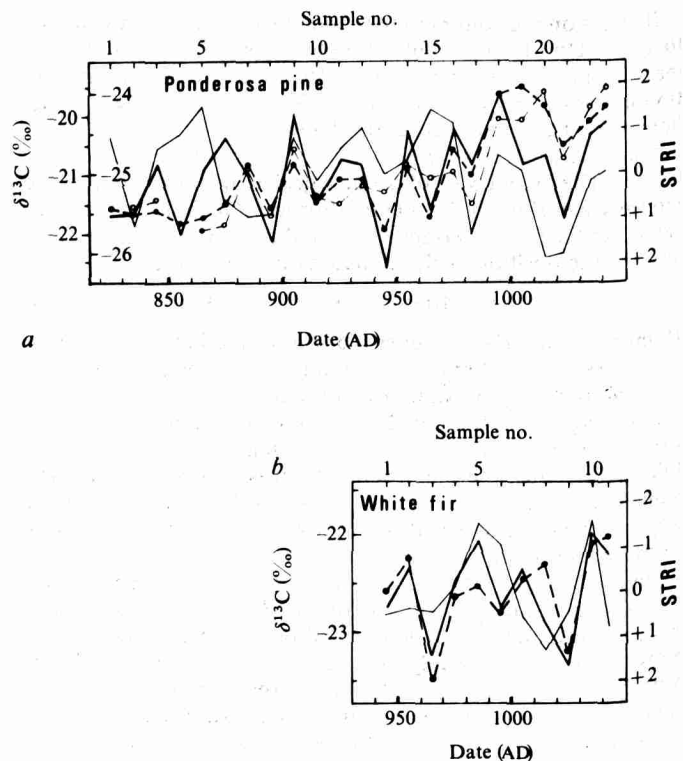


Fig. 1 Time series $\delta^{13}\text{C}$ values and tree-ring indices in the three sections from the Chetro Ketl site. All $\delta^{13}\text{C}$ values are expressed by reference to the PDB standard. The $\delta^{13}\text{C}$ scales and the STRI (standard tree ring index) scales have been normalized by subtracting to each value in a series the mean of each series then dividing it by the corresponding standard deviation. *a*, Thick line: decadal means of the Chaco Canyon regional ponderosa mean STRI. Thin line: decadal means of the individual STRI for the sampled section. Open circles: $\delta^{13}\text{C}$ (lignin) decadal values (inner scale). Solid circles: $\delta^{13}\text{C}$ (cellulose) decadal values (outer scale). *b*, Thick line: decadal means of the Chaco Canyon regional white fir mean STRI. Thin line: decadal means of the individual STRI for the samples section. Solid circles: $\delta^{13}\text{C}$ (cellulose) decadal values.

tions. In the Chaco Canyon and similar arid areas, ring-widths generally relate to climate in the following way: wide rings are produced during wet-cool years, and narrow rings during warm-dry years^{14–16}. The strength of these qualitative relationships has been discussed in statistical terms in recent work by Fritts *et al.*¹⁷.

Before we could ascertain the significance of a time series of carbon isotope values and test the potential of this method for the reconstruction of palaeoclimates, we had first to determine which chemical component of wood—cellulose or lignin—is most sensitive to climate; and second, to assess the uniformity of the isotope record by studying the δ values in different tree species from the same site and by measuring the variations in isotope values of a single set of rings around the tree circumference. We began our experiment by sampling a single radius of the ponderosa pine section. This provided 22 samples of 10 yr each and one of 6 yr, beginning at AD 820. These and later samples were ground into sawdust and extracted with benzene and ethanol in a Soxhlet extractor to remove oils, waxes, resins and other relatively mobile materials which may not be coeval with the corresponding tree ring. The extracted wood was separated into cellulose and lignin using standard chemical procedures similar to those described by Browning¹⁸. Carbon dioxide obtained from combustion of lignin or cellulose at 800 °C was analysed with an isotope ratio mass spectrometer (Micromass 602C) with an overall precision better than 0.1%. The results are shown in Table 1 and in Figs 1a and 2a. (In the discussion that follows we give the correlation coefficients *r* as well as their values adjusted to remove the trends reflected by the first-order autocorrelations. These adjusted values are given